JOURNAL OF MATERIALS SCIENCE 18 (1983) 593–598

Diffusion studies of porous materials

Part 3 *Effects of thermal and radiolytic oxidation on the pore structure of an AGR moderator graphite*

J. D. CLARK, M. D. McVEY, S. MURAD, P. J. ROBINSON
Department of Chemistry, Manchester Polytechnic, Manchester, UK

Steady-state and transient gas diffusion measurements are reported for two series of specimens of AGR moderator graphite. One series had been oxidized radiolytically in a coolant atmosphere in the BFB experiments at Grenoble; the other series had been oxidized thermally in air at ~ 425° C. The evolution of pore structure with oxidation is followed for each series, and in particular, the changes in restricted-access pore (RAP) volume are determined. The results, together with previous data, indicate that thermal oxidation of the gilsocarbon graphite leads to a rapid increase in RAP volume due to the opening up of closed pores. In contrast, radiolytic oxidation leads to a relatively slow growth in RAP volume due mainly to the oxidation of existing RAPs in which the coolant's methane inhibitor is substantially depleted.

1. Introduction

In previous work we have investigated the transient elution of methane into a nitrogen carrier gas [1] from the pores of a series of porous materials, including a "high reactivity" nuclear reactor graphite [2], porous polymers, concretes and sandstones [3]. The present work is concerned with measurements on the impregnated gilsocarbon graphite used in the majority of British AGR power reactors. Measurements have been made on both radiolytically and thermally oxidized specimens and a specific objective was to investigate changes in the RAP (restricted access pore) volume during the different conditions of oxidation. Such comparisons were thought to be possibly important in assessing the contribution of RAPs to the overall corrosion of the graphite structure [4–7].

2. Experimental details

The specimens for this work were provided by Springfields Nuclear Power Development Laboratory. One series had been radiolytically oxidized in the Anglo-French BFB experiments at Grenoble [8–11], and are listed in Table I with some relevant data on their history. These samples were machined after oxidation to a length and diameter of 11.1 and 7.0 mm, respectively. Thermal oxidation of the second set was carried out slowly in air at ~ 425° C, and the surface layers were turned off to produce the samples for measurement; they had a length of 10.0 mm and a diameter of 8.0 mm. The OPV, CPV and diffusivity values measured at SNPDL on these specimens are given in Table I.

Transient elution measurements were carried out as described by Clark *et al.* [1, 2] and fitted to the "modified GKF" equation as before [2]. As illustrated previously [1], fits were virtually exact (e.g. Fig. 1), and the derived pore-structure

TABLE I Data provided by SNPDL on radiolytically oxidized specimens

Specimen identity	% Weight loss*		
	CO_2	Inhib.	Total
A	–	5.8	5.8
B	2.3	6.5	8.8
C	10.2	2.8	13.0
D	–	17.7	17.7
E	4.6	16.1	20.7
F	–	23.1	23.1

*"CO_2" = % wt loss in pure CO_2 coolant. "Inhib." = % wt loss in inhibited coolants (approximate composition 2.05 vol% CO, 200 vpm methane, 220 vpm water, 300 vpm hydrogen).

0022–2461/83/020593–06$03.22/0

TABLE II Summary of pore structure parameters

Specimen	% wt loss*	Steady-state results				Transient Elution Results (this work)									
		OPV(%) (SNPDL)	CPV (%) (SNPDL)	λ (SNPDL)	λ (Present work)	λ	OPV (%)					RAP time constants		Tortuosity, τ	Fractional pore area, α
							Total	Φ_1	Φ_2	Φ_3	$\Phi_2 + \Phi_3$	$10^3\ Y_2$ (sec^{-1})	$10^4\ Y_3$ (sec^{-1})		
M	virgin	–	–	0.007	0.006	–	–	–	–	–	–	–	–	–	–
N	virgin	11.1	8.49	0.005	–	0.003	8.4	8.2	–	0.27	0.27	–	5.70	5.2	0.016
		12.1		0.004	–	0.004	9.8	9.2	–	0.64	0.64	–	5.19	4.9	0.020
A	5.84 R	17.3	7.77	0.002	0.003	0.002	13.3	11.7	0.51	1.06	1.66	1.31	2.10	7.7	0.015
						0.002	13.8	12.0	0.55	1.32	1.87	1.68	2.08	7.7	0.016
B	8.81 R	19.1	7.38	0.008	0.007	0.004	17.3	15.4	0.65	1.24	1.89	1.73	2.38	6.6	0.023
						0.004	18.4	17.4	0.34	0.69	1.03	1.71	2.32	6.6	0.027
C	13.0 R	23.0	6.72	0.011	–	0.014	21.7	19.9	0.61	1.19	1.90	2.88	3.14	3.8	0.053
D	17.7 R	27.6	5.65	0.019	–	0.018	23.6	21.9	0.56	1.13	1.69	2.85	3.74	3.7	0.060
E	20.7 R	30.1	5.43	0.026	–	0.028	30.6	28.8	0.65	1.14	1.79	2.69	3.02	3.2	0.089
F	23.1 R	32.6	4.98	0.032	0.043	(0.033)†	(25.1)†	(24.0)†	0.23	0.86	1.09	2.03	2.42	2.7	0.089
						0.036	28.7	28.0	0.21	0.57	0.78	2.98	2.36	2.8	0.101
U	1.5 T	16.0	5.27	0.006	–	0.004	17.8	15.7	0.66	1.39	2.05	1.39	2.22	6.0	0.026
V	1.6 T	16.4	5.06	0.006	–	0.003	14.1	12.1	0.60	1.46	2.06	1.67	2.29	6.2	0.020
W	5.4 T	20.2	3.81	0.010	–	0.001_3	7.6	4.5	1.62	1.46	3.08	2.10	1.93	5.8	0.008
X	10.5 T	25.7	2.89	0.020	–	0.016	24.4	20.0	1.15	3.19	4.34	0.47	0.84	3.5	0.057
						0.018	27.3	23.9	2.36	1.04	3.40	5.88	5.34	3.7	0.065
Y	14.7 T	27.3	2.60	0.056	–	0.029	31.7	29.9	0.42	1.37	1.79	1.63	15.0	3.2	0.093
						0.025	27.2	25.0	0.45	1.79	2.24	2.50	2.17	3.1	0.079

*R = Radiolytically oxidized, present work; T = thermally oxidized [3].

†Using time offset 0.08 min (see Table III).

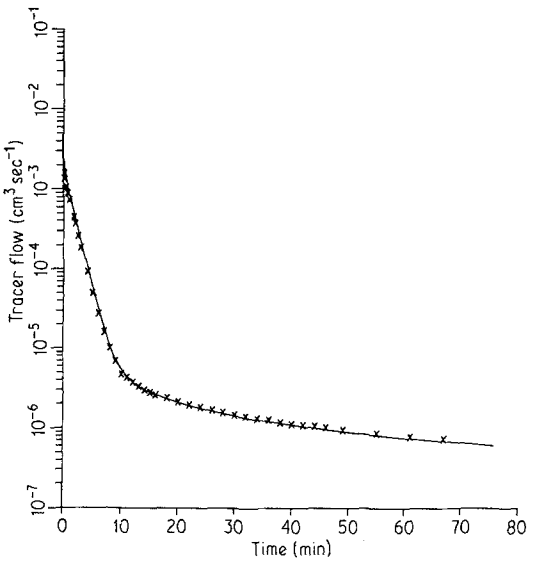

Figure 1 Transient elution plot for Specimen B.

parameters are summarized in Table II. Steady-state diffusivity measurements using methane/nitrogen [1, 3] were also carried out on some of the specimens, for comparison with the SNPDL values; the results are included in Table II. All measurements were made at a temperature of approximately 52° C unless stated otherwise. The quantities in Table II are as follows: λ = diffusivity; Φ_1 = fractional OPV in transport pores; Φ_2, Φ_3 = fractional OPV in RAPs with time constants Y_2 and Y_3, respectively; τ = tortuosity (of transport pores), $(\Phi_1/\lambda)^{1/2}$; α = apparent transport pore fractional cross-sectional area, $(\Phi_1\lambda)^{1/2}$; L = specimen length.

3. Discussion

The steady-state diffusivities measured at SNPDL and at Manchester Polytechnic are in good agreement, even where the trend with oxidation is unexpected (e.g. specimens M, A, B). The apparatus and analytical techniques are completely different, and the agreement provides a good measure of confidence in the results obtained.

Excellent fits were obtained of the GKF-based theory [1] to the experimental elution results. In optimizing these fits, all the ϕ_i, Y_i and λ were allowed to vary without constraint (λ being incorporated in the parameter $Y_1 = \lambda D\pi^2/\Phi_1 L^2$). Satisfactory fits were usually obtained with a total OPV ($\Phi_1 + \Phi_2 + \Phi_3$) which was somewhat lower than the helium OPV (see Table II). This has previously been attributed to the initial elution from the dead-space; very small errors in this section of the curve can alter the optimized parameters quite significantly. In one case only, Transient Run 1 on specimen F, the optimized fit gave an OPV which was impossibly low (Table III, time error zero). A possible source of error was a faulty start to the run, giving effectively a shift in the time axis. Computer fits were therefore carried out to modified data with the times all incremented by 0.02 to 0.08 min. Perfectly acceptable fits were obtained in all cases, and Table III shows that time errors of this order (only 5 sec) can shift the OPV into the correct region.

These results confirm our previous conclusion that the Φ_1 values from the transient results are not particularly reliable, and since λ and Φ_1 are connected, similar remarks apply to the λ values from the transients. In the remainder of the discussion, we therefore use the steady-state λ values and calculate the transport pore volume as $\Phi_1 = \epsilon - \Phi_2 - \Phi_3$, using the pyknometer OPV for ϵ. In contrast, the results show that the data for the RAPs are quite insensitive to errors of the type discussed, since the values for Φ_2, Φ_3, Y_2, Y_3 in Table III are effectively constant. Since the main object of the technique is characterization of RAP structures, this is very encouraging.

As in previous work, we find that the RAP volume in these graphites is relatively small and does not change enormously in absolute terms upon oxidation under any of the conditions studied. Under these circumstances, any discussion is confused by the inherent variability of graphite

TABLE III Effect of time error for specimen F, Run 1. (Pyknometer OPV 32.6%)

Assumed time offset (min)	OPV (%)				Time constants	
	Total	Φ_1	Φ_2	Φ_3	$10^3\ Y_2$ (sec^{-1})	$10^4\ Y_3$ (sec^{-1})
0.00	13.23	12.14	0.21	0.88	2.02	2.39
0.02	14.16	13.06	0.22	0.88	2.12	2.27
0.04	14.91	13.80	0.24	0.86	1.87	2.22
0.06	22.82	21.74	0.25	0.85	1.75	2.25
0.08	25.11	24.02	0.23	0.86	2.03	2.42

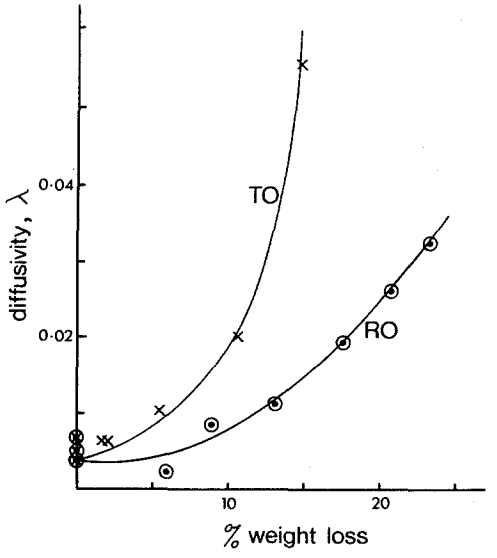

Figure 2 A plot of diffusivity, λ, against % weight loss; TO = thermal oxidation, RO = radiolytic oxidation.

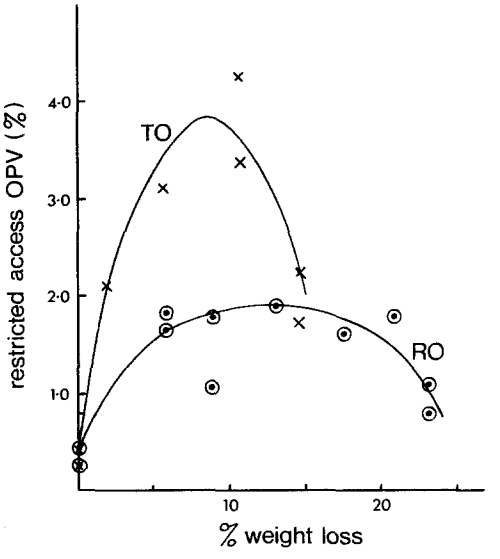

Figure 4 A plot of % RAP volume ($\Phi_2 + \Phi_3$) against % weight loss.

characteristics from specimen to specimen; for example Specimens A and W appear to be somewhat "abnormal". In this context, there are no discernable differences between specimens oxidized in inhibited or partly in uninhibited coolants; any distinction must be small and masked by the general scatter of results. Despite any limitations, however, relative changes can be discerned and will provide a useful insight into the evolution of the pore structure with oxidation.

In Figs. 2 to 6 various pore structure parameters are plotted against % weight loss. It is immediately apparent that these plots are different for thermal (TO) and radiolytic (RO) oxidation. For example, the RAP volume increases during the first 10% weight loss in both cases, but much more so for TO than RO (Fig. 4). Similarly the diffusivity (Fig. 2) and tortuosity (Fig. 5) vary in a significantly different way for the two types of oxidation.

This difference, which is at first sight puzzling, can be rationalized by a consideration of the closed pore volume (CPV) (Fig. 7). As has been noted by other workers [12] the CPV of gilsocarbon graphite is opened up more rapidly by TO than by RO. This is shown in Fig. 7 by (a) a more rapid decrease in CPV, and (b) a more rapid

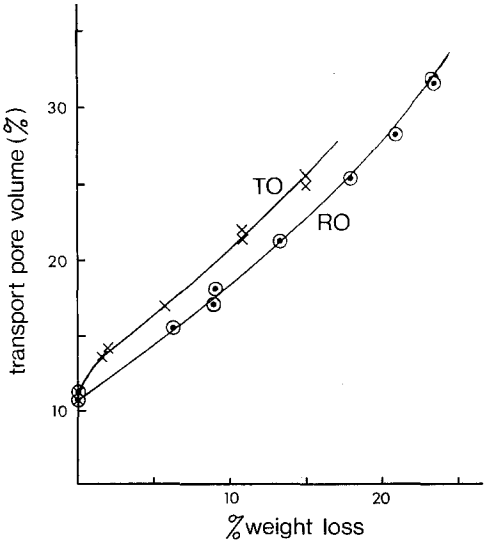

Figure 3 A plot of % transport pore volume ($\epsilon - \Phi_2 - \Phi_3$) against % weight loss.

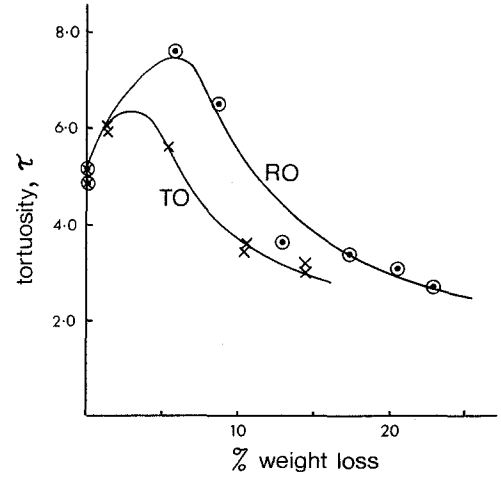

Figure 5 A plot of tortuosity, τ, against % weight loss.

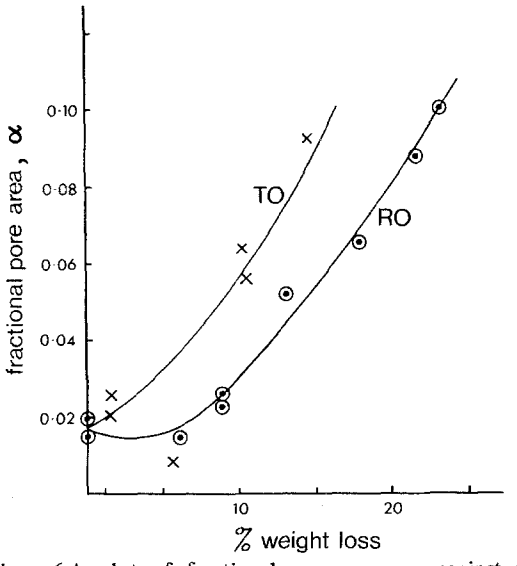

Figure 6 A plot of fractional pore area, α, against % weight loss.

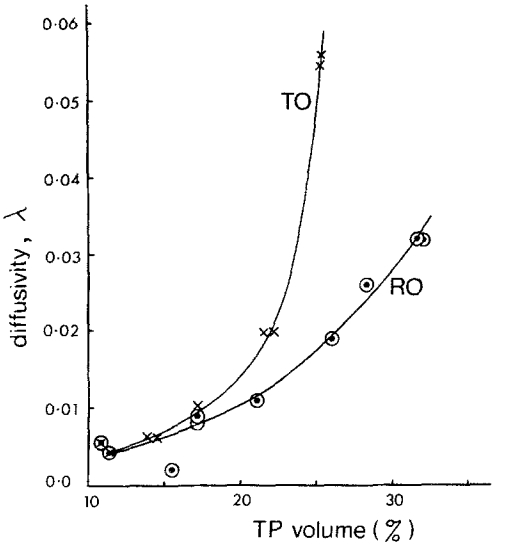

Figure 8 A plot of diffusivity, λ, against % transport pore volume.

increase in total OPV with per cent weight loss by TO.

The present results demonstrate unequivocally what had previously been a resonable hypothesis, that the CPV which is opened up by TO is converted to a major extent into RAPs (Fig. 4).

Since a significant proportion of the new OPV is in RAPs, the transport properties would be better related to TP volume Φ_1 rather than % weight loss or total OPV. Again the present results provide new information which makes this possible, and appropriate plots are shown in Figs. 8 to 10.

Although there are still differences between RO and TO, they are much less marked when the comparisons are made at a given TP volume rather than a given total % weight loss.

It is potentially instructive to analyse the changes in volume in an attempt to define what processes are occurring during the oxidation. Such an analysis is likely to be simplest in the initial stages of the oxidation. Table IV compares the changes in volume (expressed as percentage of the specimen volume) accompanying 1.6% TO and (interpolated) 2.2% RO, chosen to give the same

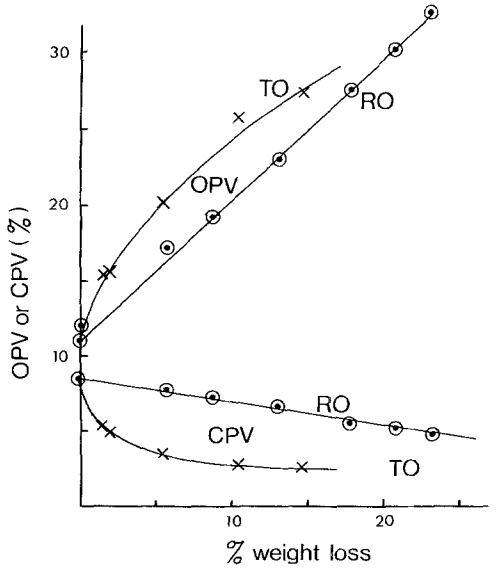

Figure 7 A plot of % OPV and CPV against % weight loss.

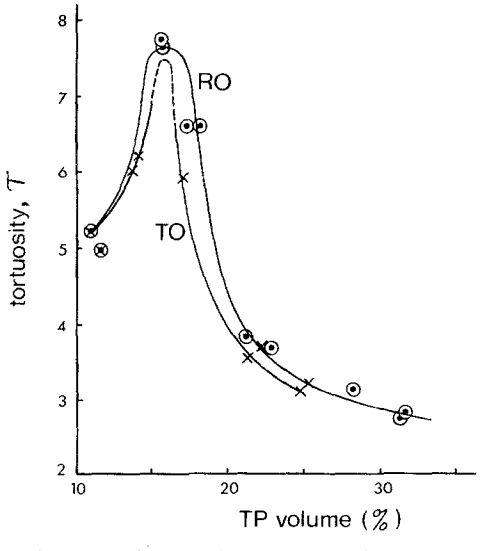

Figure 9 A plot of tortuosity, τ, against % transport pore volume.

TABLE IV Volume changes accompanying 1.6% TO and 2.2% RO

	TO		RO	
Increase in volume due to C loss	1.9%	5.3%	1.8%	2.1%
CPV opened up	3.4%		0.3%	
Increase in RAP volume	1.7%	5.3%	0.7%	2.1%
Increase in TP volume	3.6%		1.4%	

apparent volume increase due to carbon removal (the change in vol % C = 100 − OPV − CPV).

The data in Table IV are consistent with the well-established model in which RO takes place predominantly in the RAPs in a well-ventilated specimen, whereas TO takes place throughout the pore structure. It is evident that in the gilsocarbon graphite TO at impurity sites creates "tunnel pores" [12] from the TPs into the CPV, thus creating RAPs (by one tunnel pore) or more TP volume (by two or more tunnel pores). The CPV which is opened up appears to divide equally into RAP and TP volume. In contrast, RO results in relatively little opening-up of CPV and the RAP volume grows more by enlargement of existing RAPs, as found for a more open-pored nuclear graphite [1]. These conclusions are consistent with (a) protection of TPs but not RAPs by methane in the RO experiments, and (b) the catalytic effect of impurities in the TO but not the RO experiments. In the TO experiments with the open-pored graphites, the RAP volume decreased rather than increased, consistent with the absence of CPV to be opened up in this material [1].

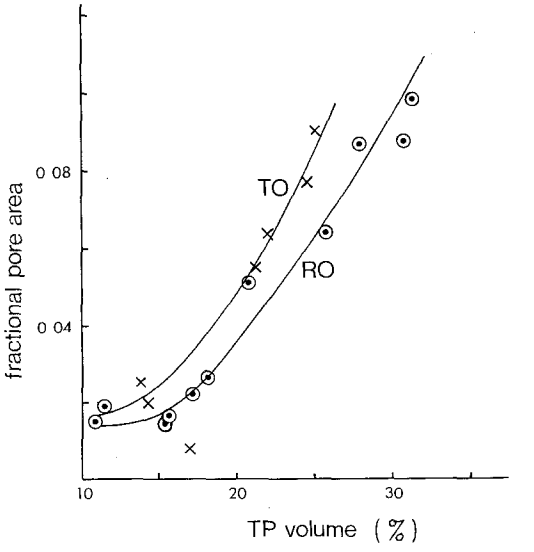

Figure 10 A plot of fractional pore area, α, against % transport pore volume.

In conclusion, the present results complete another aspect of the investigation of the pore structure of oxidized graphites, and are consistent with the emerging picture of the factors controlling the radiolytic and thermal oxidation of different materials. In particular, the pore-structure model can now incorporate factual quantitative information on the magnitude and the evolution of the restricted-access component of the open pore volume.

Acknowledgements

We are grateful to the UKAEA (Springfields Nuclear Power Development Laboratory) for financial support and for permission to publish this work, to the SERC for a studentship (MDM), and to the staff of SNPDL for numerous helpful discussions.

References

1. J. D. CLARK, C. S. GHANTHAN and P. J. ROBINSON, *J. Mater. Sci.* **14** (1979) 2937.
2. J. D. CLARK and P. J. ROBINSON, *ibid.* **17** (1982) 2649.
3. M. D. McVEY, M.Phil thesis (CNAA) (1981).
4. A. DYER (ed), "Gas Chemistry in Nuclear Reactors and Large Industrial Plant" (Heyden, London, 1980).
5. J. V. SHENNAN, *ibid.* "Radiolytic Carbon Gasification", p. 98.
6. A. BLANCHARD, *ibid.* "Development of Transport and Non-Transport Porosity in Radiolytic Graphite Oxidation", p. 134.
7. J. V. BEST, *ibid.*, "Modelling of AGR Radiolytic Graphite Corrosion", p. 141.
8. P. CAMPION, A. BLANCHARD, R. LIND, R. J. BLANCHARD and C. KOCH, in "Proceedings of the 4th London International Conference on Carbon and Graphite", (Society of Chemical Industry, London, 1976) p. 452.
9. P. CAMPION, R. LIND, R. J. BLANCHARD and C. KOCH, *ibid*, p. 459.
10. P. CAMPION, A. BLANCHARD, J. KETCHEN and P. SCHOFIELD, in "Proceedings of the 14th Biennial Conference on Carbon", (Pennsylvania State University, Pennsylvania, 1979) p. 449.
11. A. BLANCHARD, J. KETCHEN, P. SCHOFIELD and P. CAMPION, in "Gas Chemistry in Nuclear Reactors and Large Industrial Plant", edited by A. Dyer (Heyden, London, 1980) p. 129.
12. P. SCHOFIELD, B. FITZGERALD and P. CAMPION, Conference on Recent Advances in the Physics and Chemistry of Carbon and its Applications, Salford, September 1981.

Received 2 June
and accepted 16 July 1982